

Research Article

Parallel middle body lengthening for high speed craft: A machine learning supported framework

Muhammad Raafie Caesar Putra Hadi*, Deddy Chrismianto, Ahmad Firdhaus and Eko Sasmito Hadi

Department Naval Architecture, Faculty of Technology, Diponegoro University, Tembalang, Semarang, Central Java 50275, Indonesia

*Corresponding author's e-mail address: mraafliel@gmail.com

Article information

Received: November 1, 2025
Revision: January 13, 2026
Accepted: February 2, 2026

Keywords

Parallel middle body (PMB);
Fast passenger monohull;
Hydrostatics and stability;
Longitudinal strength;
Resistance prediction;
Machine learning surrogate;
Gradient Boosting

Abstract

Fast passenger craft play a strategic role in maritime transport, yet early-stage hull-form modifications are often constrained by competing requirements in resistance, stability, and structural strength. Rather than pursuing a clean-sheet redesign, this study adopts parallel middle body (PMB) lengthening as a controlled intervention that preserves validated bow-stern geometry and is compatible with practical retrofit and construction constraints. A fast passenger monohull is incrementally lengthened from 29.8 to 35.8 m through PMB extension, generating 61 variants in 0.10 m steps; the maximum 6 m increase reflects supplier limits on modular insert fabrication and the need to avoid extensive reconfiguration of internal systems (e.g., piping routes). For each variant, hydrostatics, intact transverse stability, longitudinal strength, and calm-water resistance/running attitude are evaluated using a semi-empirical framework; resistance is assessed at the service condition and through a Froude-number sweep ($Fr = 0.10 - 0.40$) for regime-based interpretation. The results show consistent improvements in hydrostatics and stability, smoother longitudinal load distributions, and reduced total resistance at the target operating condition, primarily driven by lower residuary resistance. To accelerate design-space exploration, supervised-learning surrogates are benchmarked across five regressors, with ensemble methods, particularly Gradient Boosting, providing the highest predictive fidelity for nonlinear performance trends. A multi-criteria ranking-and-scoring procedure identifies an optimal length of 35.4 m, balancing resistance reduction with stability enhancement and strength compliance. Overall, the PMB machine learning (ML) framework offers an efficient and transparent pathway for early-stage decision making in high-speed monohull design.

1. Introduction

High-speed passenger craft occupy a distinctive and challenging design regime wherein hydrodynamic performance, safety margins, and regulatory compliance must be simultaneously satisfied under increasingly stringent economic and environmental pressures. As operational envelopes extend into semi-displacement and planing regimes, marginal alterations in hull geometry can precipitate disproportionately large variations in resistance, trim, and stability characteristics. Classical empirical approaches, most notably the Savitsky family of formulations, continue to provide utility in conceptual design due to their computational efficiency and accessibility. However, their applicability is increasingly challenged by modern geometrical features such as warped bottoms, appendages, and novel stern configurations, which can lead to significant fidelity losses (Hetharia et

al., 2021; Paredes et al., 2023). Computational fluid dynamics (CFD), by contrast, has achieved sufficient maturity to replicate experimental benchmarks for resistance and motions with high fidelity, albeit at considerable computational cost and limited throughput (Avci & Barlas, 2018; Khazaei et al., 2019). This dichotomy underscores the need for surrogate strategies, particularly those employing machine learning (ML), to reconcile the trade-off between breadth of coverage and depth of accuracy in early-stage design.

A substantial body of maritime literature highlights resistance and speed-power prediction as central determinants of fuel efficiency, emissions, and overall vessel operability. Data-driven models, ranging from ensemble methods to deep neural networks, have demonstrated reliable predictive capacity when trained on sensor-derived datasets or curated repositories (Bassam et al., 2022; Lang et al., 2022a). Complementary research emphasizes the tension between predictive accuracy and interpretability, giving rise to physics-informed ML strategies that integrate hydrodynamic priors into learning architectures (Lang et al., 2021; Schirmann et al., 2023). Meanwhile, emerging databases, such as SHIP-D, address the chronic paucity of open hull-performance data, thus enabling broader application of surrogate modeling and optimization pipelines (Bagazinski & Ahmed, 2023).

The focal research question in this work is whether incremental hull lengthening can be systematically exploited to improve resistance performance and enhance stability margins at high service speeds, while maintaining acceptable structural integrity. Lengthening modifies slenderness ratios (e.g., length-to-beam (L/B)) and displacement-to-length relationships that directly mediate residuary and viscous resistance components, as well as intact stability envelopes (Le et al., 2023). Yet, these modifications are inherently non-monotonic: while increased length generally reduces residuary resistance, it simultaneously elevates wetted surface and frictional penalties, alters trim and sinkage, and potentially redistributes hydrostatic loads in ways that affect stability and strength (Baso et al., 2020; Montero & Valentina, 2017). Addressing these interactions requires an integrative framework spanning hydrodynamics, intact stability, and structural analysis, as opposed to treating these domains in isolation (Temple & Collette, 2016).

Traditional design pipelines rely heavily on empirical estimators derived from systematic series, occasionally complemented by physical model tests where resources permit. Despite their expedience, Savitsky-type predictions often deviate at higher Froude numbers or when unconventional geometries are introduced (Hetharia et al., 2021; Soma & Vijayakumar, 2023). CFD provides improved fidelity, but is computationally prohibitive for densely populated design spaces (Avci & Barlas, 2018; Baso et al., 2021). These limitations motivate hybrid approaches in which inexpensive physics-based estimators and selective CFD calculations are combined to generate compact but high-quality datasets used to train ML surrogates capable of interpolating across neighboring variants (Ferlita et al., 2024a; Ferlita et al., 2024b).

Within the preliminary stages of ship design, parallel middle body (PMB) extension presents a strategically viable alternative to complete hull redevelopment. As a controlled parametric modification, PMB elongation preserves geometric continuity and hull fairness while facilitating targeted analysis of longitudinal geometric influences (Brizzolara et al., 2015; Villa et al., 2020). These incremental interventions demand fewer computational, engineering, and certification resources than comprehensive redesign, yet still yield measurable improvements in hydrodynamic and structural performance (Peri & Campana, 2005; Temple & Collette, 2016). By leveraging pre-validated bow and stern configurations, PMB extensions reduce the risk associated with novel hull forms and ensure compatibility with existing construction and classification protocols (Gafer & Drimer, 2021). This approach enables enhancement of longitudinal characteristics, volumetric capacity, and resistance profiles without disrupting the vessel's core architectural integrity, thereby minimizing the economic, temporal, and logistical burdens inherent to clean-sheet designs (Salazar-Domínguez et al., 2021). In practical terms, constraints related to shipyard capabilities, dimensional regulations, and route-specific requirements further underscore the appropriateness of PMB interventions, especially in high-speed craft applications (Zheng et al., 2021; Djačkov et al., 2018).

When integrated with advanced computational techniques, such as CFD and machine learning surrogates, the PMB approach enables high-resolution exploration of performance trends within a narrowed design space, while maintaining methodological transparency and reducing uncertainty (Elkafas et al., 2021). It is acknowledged, however, that PMB extension is not a comprehensive substitute for full multi-variable optimization. Rather, it is best understood as a focused refinement strategy, tailored for constrained early-stage design contexts requiring modular and tractable interventions.

Several lines of prior research foreshadow the methodology employed here. Parametric RANS studies corroborated by experimental data reveal that increasing L/B ratios typically attenuate pressure-resistance components, though effects on viscous resistance remain nuanced (Le et al., 2023; Khazaei et al., 2019). Appendage-based interventions, including stern flaps, interceptors, and hull vanes, demonstrate measurable reductions in trim and resistance, yet their efficacy is highly geometry and Froude-dependent (Soma & Vijayakumar, 2023; Samuel et al., 2024). Planing and semi-planing craft studies further underscore the sensitivity of trim-by-stern behavior and center-of-gravity placement, both of which yield complex trade-offs between resistance minimization and intact stability ranges (Baso et al., 2020; Wang et al., 2023).

The machine learning literature complements these naval architectural findings by showcasing regression surrogates, particularly Gradient Boosting, XGBoost, and neural networks, which effectively emulate resistance, powering, and motion performance when paired with rigorous preprocessing and validation protocols (Bassam et al., 2022; Bassam et al., 2023; Fan et al., 2024). Hybrid physics data models mitigate extrapolation risk by embedding hydrodynamic structure into the learning process, thereby improving generalizability beyond the training distribution (Ahn et al., 2022; Kanazawa et al., 2023). Increasingly, explainable AI techniques are applied to maritime ML tasks, balancing predictive strength with transparency in feature attribution (Schirrmann et al., 2023; Barhrhouj et al., 2025). Together, these advances indicate that ML is poised to become integral to concept design workflows.

This study, therefore, develops an integrated, data-driven pipeline for evaluating finely spaced PMB-based lengthening variants of a fast passenger monohull with fixed principal particulars. Specifically, the analysis spans Length Over Hull from 29.80 m elongated to 35.80 m, in 10 cm increments, while Breadth Moulded (5.20 m), Depth Moulded (2.50 m), and Draft (1.25 m) are held constant.

Empirical and semi-empirical formulations are applied to rapidly screen hydrostatics, stability, strength, and resistance characteristics across the design space, supplemented where necessary by higher-fidelity computations. The dataset is then employed to train regression surrogates emphasizing ensemble learners such as Gradient Boosting, validated through cross-validation against performance metrics (Lang et al., 2022a; Lang et al., 2022b; Fan et al., 2024). The surrogates enable continuous interpolation across length variants, supporting a multi-criteria synthesis that balances reductions in resistance against gains in GMt, righting-arm areas, and structural robustness. This methodological integration directly aligns with contemporary design for operations paradigms that prioritize energy efficiency alongside safety and compliance (Temple & Collette, 2016; Garbatov & Huang, 2020).

A closer examination of related work highlights the unresolved research gap. Optimization studies for high-speed craft traditionally integrate parametric hull manipulations, heuristic search, and empirical estimators, sometimes augmented by surrogates to reduce reliance on costly solvers (Mohamad Ayob et al., 2010; Wang et al., 2021). More advanced approaches have explored multi-objective and reliability-based optimization, including Pareto-front analyses and hierarchical decompositions (Ma et al., 2016; Garbatov & Huang, 2020). However, few contributions systematically interrogate incremental PMB lengthening as a single-parameter lever with

implications across hydrodynamics, intact stability, and structural integrity, while simultaneously embedding ML surrogates calibrated on dense, systematically generated design variants. Furthermore, while numerous studies investigate propulsion power and energy modeling, fewer examine fine-grained geometric modifications in the order of 0.10 m resolution coupled with ML-supported multi-criteria optimization for specific high-speed service conditions (Bagazinski & Ahmed, 2023; Ferlita et al., 2024b).

Accordingly, the dual objective of this paper is: (i) to quantify the impact of incremental PMB-based lengthening on hydrostatics, transverse stability, longitudinal strength, and resistance of a fast passenger monohull at service speed, and (ii) to demonstrate that ML surrogates, when validated and embedded in a structured decision framework, can identify an optimal length that reconciles these competing design drivers. The novelty lies in combining fine-resolution parametric variation with multi-domain naval architectural assessment and transparent ML-enabled ranking. The present scope is deliberately constrained to calm water performance, intact stability, and longitudinal strength, with seakeeping, appendage interactions, and life-cycle operational factors identified as extensions for subsequent investigation. By reconciling empirical rapidity, selective high-fidelity accuracy, and surrogate generalization, this study contributes a structured, doctoral-level perspective on early-stage hull-form refinement for high-speed passenger vessels (Lang et al., 2022b; Temple & Collette, 2016). To achieve this, the study employs parallel middle body (PMB) extension, wherein additional midbody sections of constant cross-section are inserted between fore and aft shoulders. This controlled manipulation preserves beam, depth, and entrance/run forms, thereby isolating the effects of length on hydrostatics, stability, resistance, and structural strength while maintaining hull fairness. This methodological clarity makes PMB extension an ideal testbed for rigorous parametric and surrogate-assisted design exploration.

2. Methodology

2.1 Baseline vessel and design space

This investigation considers a high-speed passenger monohull subjected to systematic length augmentation via parallel middle body (PMB) extension. The baseline hull of 29.8 m was incrementally extended to 35.8 m in uniform 0.10 m steps, yielding 61 variants. Throughout this process, principal dimensions aside from length, namely beam, depth, propulsion system, and appendage configuration, were preserved to ensure that length was the sole variable under examination. The geometric transformations were executed in a naval architectural CAD and analysis environment, enabling consistent recomputation of hydrostatics and downstream responses across all variants. PMB elongation was selected because it is a classical parametric modification that maintains hull fairness while isolating the effects of lengthening on performance domains (Brizzolara et al., 2015; Zhang & Mao, 2009; Villa et al., 2020). The methodological scope was confined to calm water assessments at a representative high-speed service condition, aligning with the study’s intent to examine resistance, stability, and strength in early design stages.

Figure 1 illustrates the PMB extension scheme, while **Table 1** presents the principal dimensions of the fast passenger monohull, encompassing the length variation from 29.8 to 35.8 m.

Table 1 Main particulars of the modified fast passenger vessel.

Length Over Hull	29.8 - 35.8 m
Breadth Moulded	5.2 m
Depth Moulded	2.5 m
Draft	1.25 m

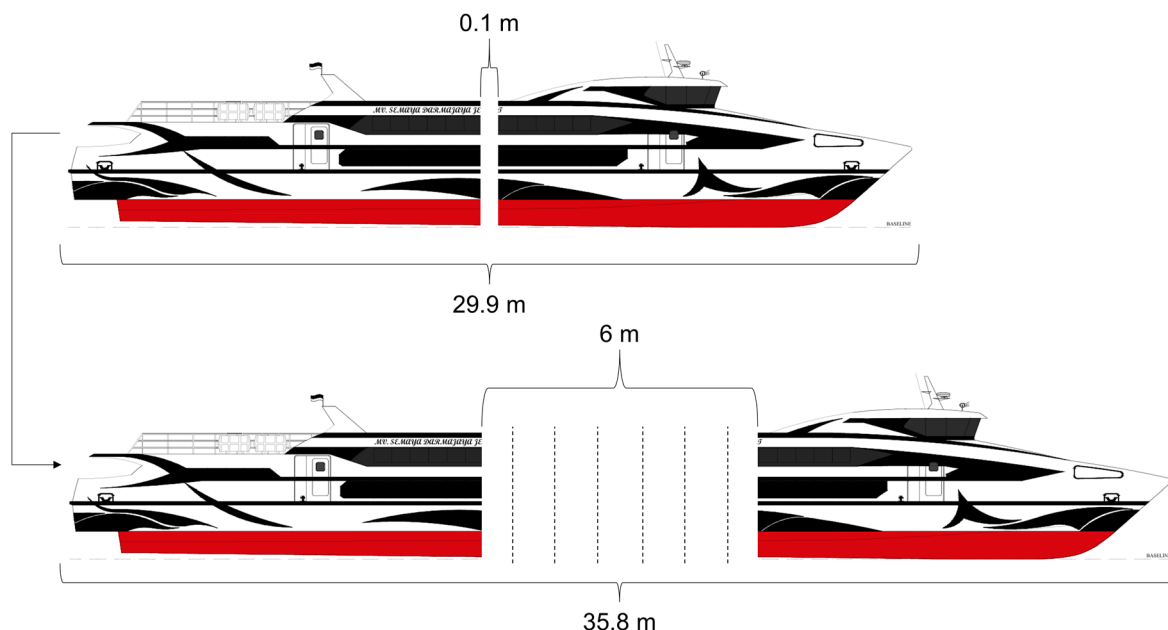


Figure 1 Schematic of 0.10 m parallel middle body (PMB) extension increments from 29.8 to 35.8 m PMB lengthening strategy applied to the baseline hull.

2.2 Hydrostatics and transverse stability evaluation

For each variant, hydrostatic particulars including displacement, drafts, waterplane area, and form coefficients were recomputed alongside stability metrics. Transverse stability assessment emphasized metacentric height (GMt) and righting arm (GZ) curves over both small heel angles (0 - 30°) and extended ranges (>30°). This approach ensured that both initial restoring characteristics and reserve stability envelopes were systematically quantified. The procedure follows established intact-stability protocols in naval architecture, as supported by previous parametric stability investigations (Alamsyah et al., 2024; Pawłowski, 2017; Begović et al., 2020). By holding non-length dimensions constant, any observed improvements in GMt or GZ area can be attributed directly to the PMB elongation strategy.

2.3 Longitudinal strength assessment

To evaluate structural implications of hull elongation, still-water shear force and bending-moment envelopes were derived for each variant. Hydrostatic pressure distributions and representative weight distributions, appropriate to high-speed passenger craft service, were employed. The assessment emphasized comparative trends rather than detailed scantling analysis. The objective was to determine whether PMB elongation moderated peak load intensities and produced smoother internal-force distributions. This approach aligns with standard preliminary-design assessments of longitudinal strength, recognizing that advanced reliability-based frameworks exist but remain outside the present scope (Wei et al., 2019).

2.4 Resistance and running attitude estimation

Calm water resistance predictions were carried out using a semi-empirical framework suitable for semi-planing and planing regimes at high Froude numbers. The methodology decomposed total resistance into frictional and residuary components, while simultaneously solving for dynamic trim and sinkage. This procedure generated total resistance coefficients and qualitative running-attitude profiles for each variant. Although empirical in nature, such formulations deriving from Savitsky-type methods remain integral to early-stage evaluation of high-speed craft performance, despite their limitations in accounting for warped bottoms or fine-form geometries (Hetharia et al., 2021; Paredes

et al., 2023). The method enabled efficient exploration of all 61 variants, providing a dense mapping of performance trends prior to any higher-fidelity CFD or experimental campaigns.

To extend the analysis beyond a single operating condition and enable regime-based interpretation, a systematic Froude-number sweep was incorporated into the resistance estimation procedure. Total and residuary resistance coefficients were evaluated over a nondimensional Froude number range of $Fr = 0.10 - 0.40$ using uniform increments sufficient to resolve trend variations across the spectrum. For each hull-length variant, the corresponding vessel speed at a given Froude number was computed according to $V = Fr \sqrt{gL}$, where g denotes gravitational acceleration and L represents the characteristic hull length adopted consistently throughout the study. Resistance components were then calculated at these equivalent speeds using the same semi-empirical formulation (Leal-Ruiz et al., 2023). Comparisons among variants were conducted at identical Froude numbers to preserve equivalence of wave-making regimes, thereby isolating the influence of hull length on total and residuary resistance behavior and enabling explicit examination of hump-hollow features in the residuary resistance coefficient that cannot be captured through single-speed analysis alone.

2.5 Data preparation and machine learning pipeline

Outputs from hydrostatic, stability, structural, and resistance analyses were consolidated into a structured dataset containing both geometric descriptors and performance responses. The dataset underwent preprocessing, including type coercion, screening for variance deficiencies, and missing-value inspection. A standard 80/20 train test split with fixed random seed was applied to ensure reproducibility. Five supervised learning algorithms, Linear Regression, Ridge, Lasso, Random Forest, and Gradient Boosting, were benchmarked. Predictive performance was evaluated using R^2 , MAE, and MSE. In accordance with emerging practices in marine data analytics, tree-based ensembles provided superior fidelity in modeling nonlinear relations. Gradient Boosting was retained as the primary surrogate owing to its consistently higher explanatory power and lower error magnitudes across folds, corroborating findings from recent maritime ML studies (Callens et al., 2020; Zhan et al., 2022; Balas & Balas, 2025). The trained surrogate enabled continuous interpolation across the design space and facilitated rapid scenario testing for length optimization.

2.6 Multi-criteria synthesis for optimal length

Final selection of the recommended hull length was conducted through a ranking-and-scoring synthesis aggregating normalized indicators from three principal domains: (i) resistance (favoring lower C_t values), (ii) stability (favoring higher GMt and larger GZ areas), and (iii) longitudinal strength proxies. Surrogate-based predictions were cross-checked against baseline computations to preserve consistency. This integrative synthesis reflects best practices in concept-design optimization in which multiple, often competing, criteria must be reconciled transparently. While the present framework emphasizes interpretability and computational efficiency, it remains extensible toward multi-objective optimization and uncertainty-aware decision methodologies as advocated in the literature (Wei et al., 2019).

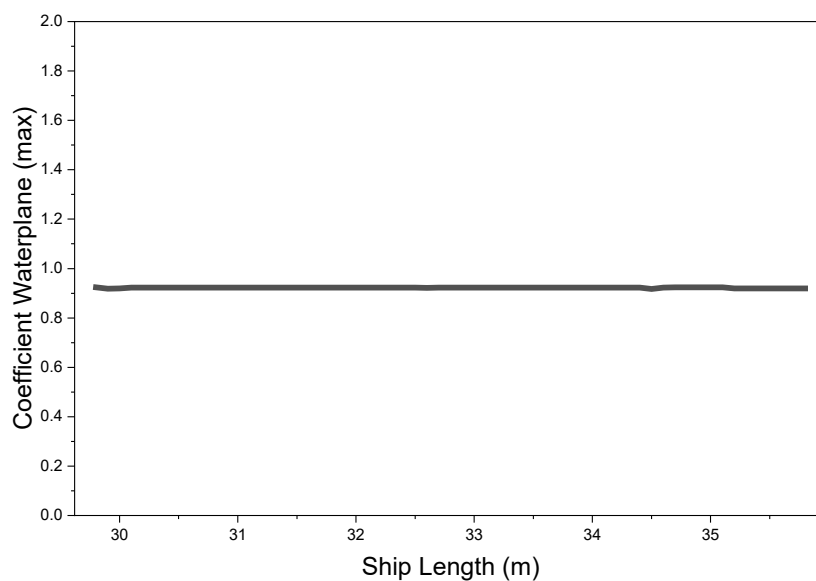
3. Results

3.1 Geometric trends and form coefficients

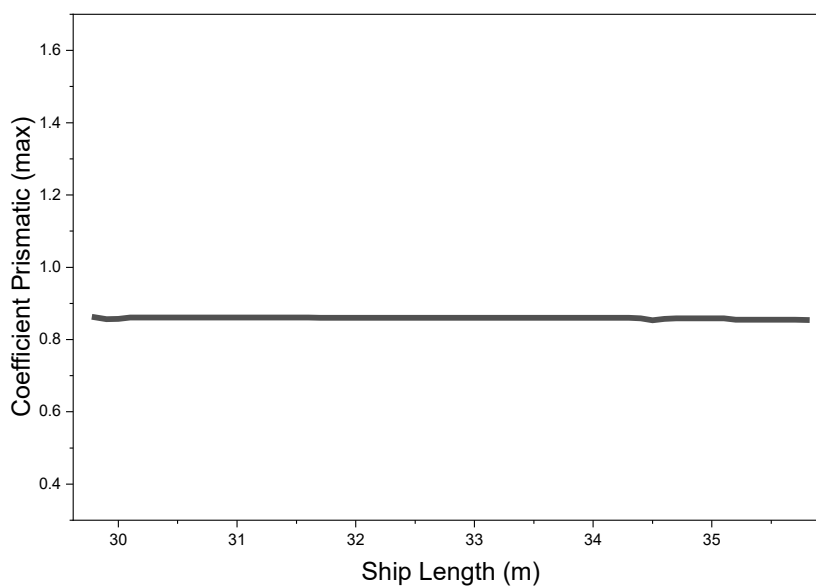
Incremental extension of the parallel middle body (PMB) induces systematic and theoretically consistent geometric transformations across the 29.8 - 35.8 m design spectrum. As length increases, the hull exhibits higher slenderness ratios (L/B , L/T), accompanied by a monotonic decline in the displacement-to-length ratio (DLR). These changes denote enhanced volumetric efficiency in regimes dominated by high Froude numbers. Concurrently, form coefficients reflect this evolution: C_w and C_p trend upward, indicating enlarged waterplane areas and fuller prismatic volumes, while C_b decreases, signaling a progressively slenderer displacement distribution.

Figure 2(a) demonstrates the progressive augmentation of C_w , which amplifies transverse waterplane stiffness and, thus, the vessel's initial stability. Similarly, **Figure 2(b)** shows the net augmentation of C_p , underscoring advantageous redistribution of longitudinal volume that moderates resistance characteristics. By contrast, **Figure 3** evidences the expected decline in C_b , reflecting hull slenderization. **Figure 4** illustrates the coherent escalation of L/B and L/T ratios, and **Figure 5** confirms the concomitant reduction in DLR, both of which are emblematic of volumetric refinement aligned with high-speed performance imperatives.

Collectively, these results affirm that PMB-based lengthening not only preserves geometric fairness but also orchestrates a volumetric redistribution conducive to reduced residuary resistance and augmented stability margins.



(a)



(b)

Figure 2 (a) Maximum waterplane coefficient (C_w) across length variants; (b) Maximum prismatic coefficient (C_p) across length variants.

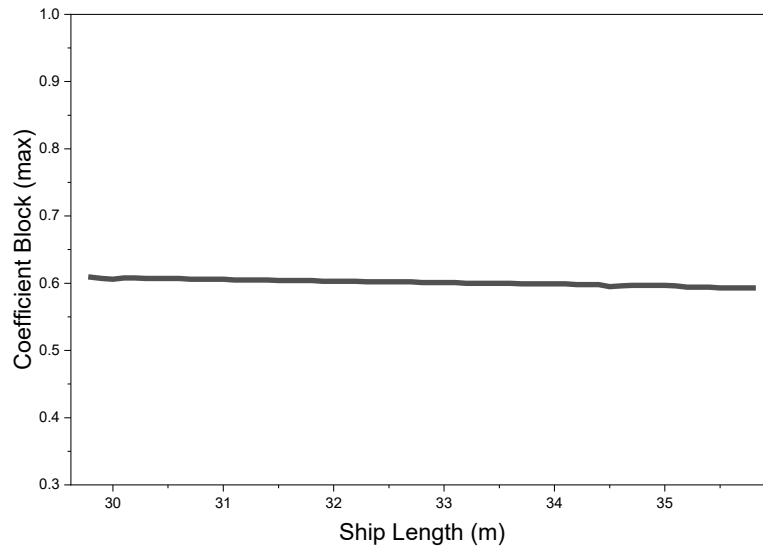


Figure 3 Maximum block coefficient (C_b) across length variants.

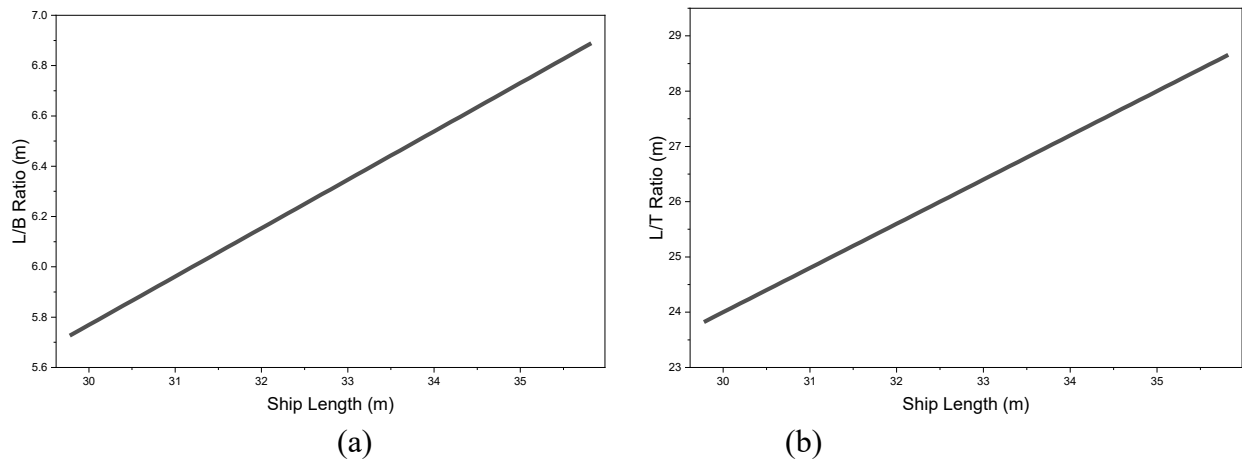


Figure 4 (a) Length-to-beam (L/B) and (b) length-to-draft (L/T) ratios by variant.

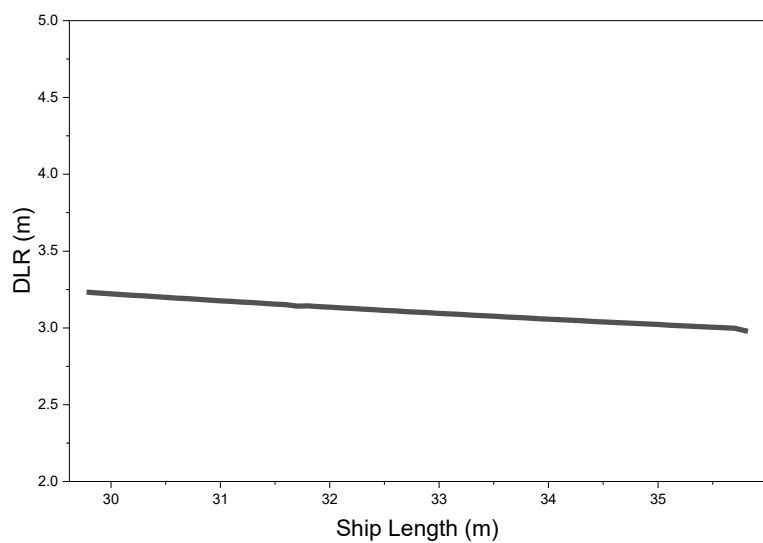


Figure 5 Displacement to length ratio (DLR) for each length variant.

3.2 Hydrostatics and stability outcomes

Hydrostatic recomputation validates that PMB elongation produces measurable enhancements in both initial and reserve stability. GMt rises consistently with length, an outcome attributable to larger waterplane moments of inertia generated by elevated C_w values. Simultaneously, righting-arm (GZ) characteristics reveal augmented curve areas across both $0 - 30^\circ$ and $>30^\circ$ heel ranges, underscoring superior restoring capacity at small angles and improved reserve stability at larger inclinations. **Figures 6, 7(a), and 7(b)** encapsulate these effects, indicating a progressive enhancement of righting energy reserves.

In narrative synthesis, these improvements harmonize with the geometric modifications identified in: greater C_w strengthens initial restoring moments, while more favorable prismatic distribution extends stability into nonlinear regimes.

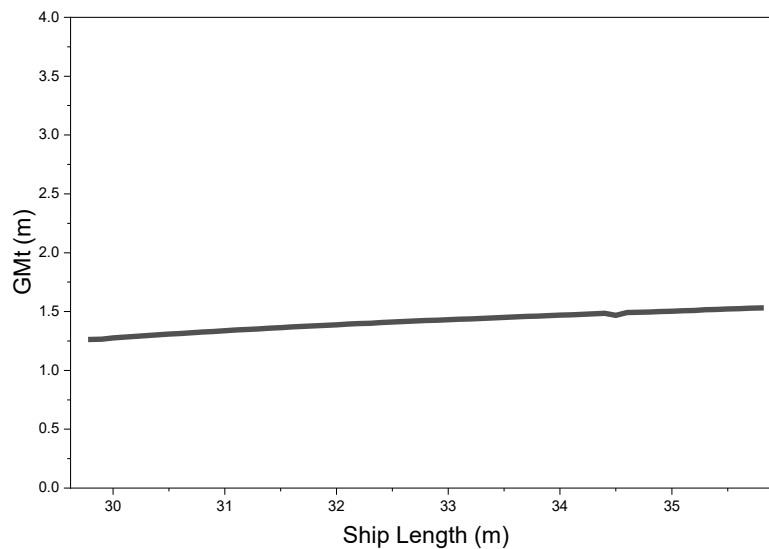


Figure 6 Transverse metacentric height (GMt) for each length variant.

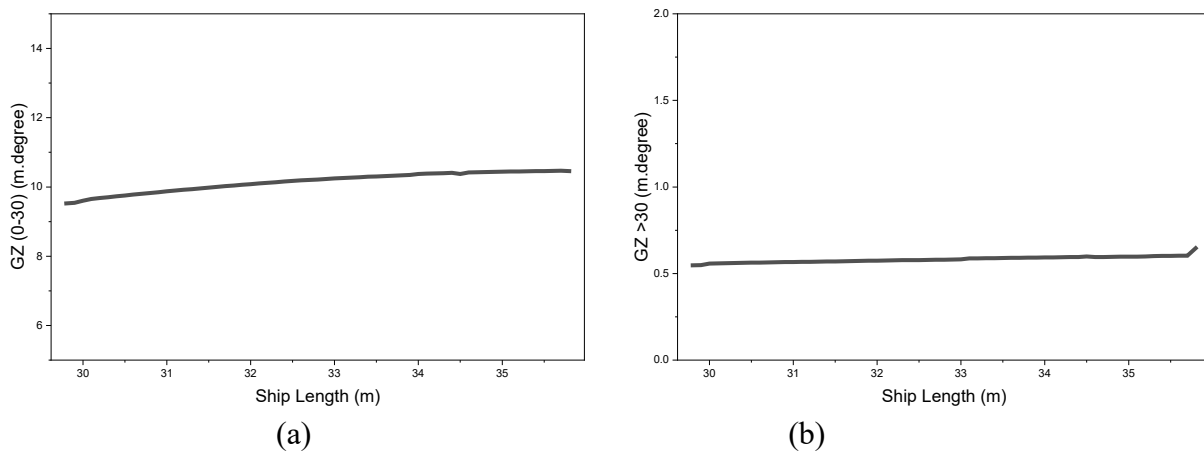


Figure 7 (a) Righting-arm area ($0 - 30^\circ$) by length variant ($m \cdot rad$); (b) Righting-arm area ($>30^\circ$) by length variant ($m \cdot rad$).

3.3 Longitudinal strength outcomes

Structural analysis indicates that PMB-based lengthening mitigates critical load concentrations. Bending-moment envelopes, exemplified in **Figure 8**, demonstrate attenuated peak magnitudes and smoother longitudinal distributions, while stress evaluations (**Figure 9**) confirm that both maximum tensile and compressive stresses remain within acceptable preliminary thresholds.

These findings corroborate prior assertions that redistribution of hydrostatic loading, rather than its escalation, governs structural response under controlled geometric modifications.

Thus, PMB extension not only avoids overloading but also reduces susceptibility to localized structural hot-spots, thereby enhancing operational robustness for high-speed service envelopes.

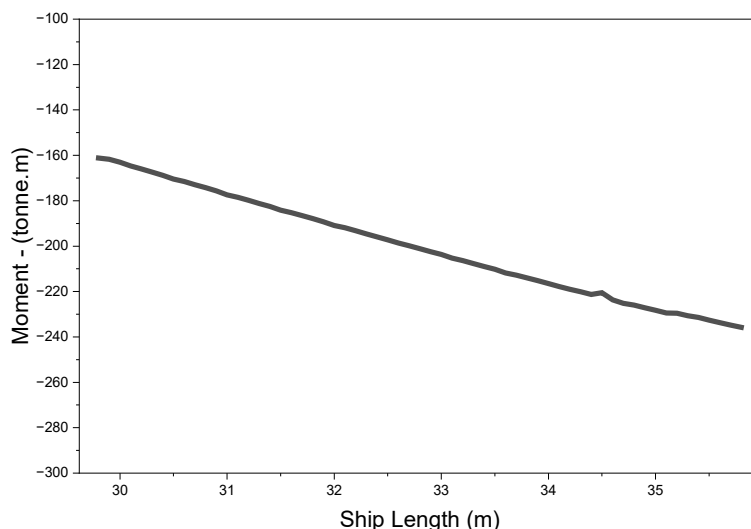


Figure 8 Still-water bending moment by length variant.

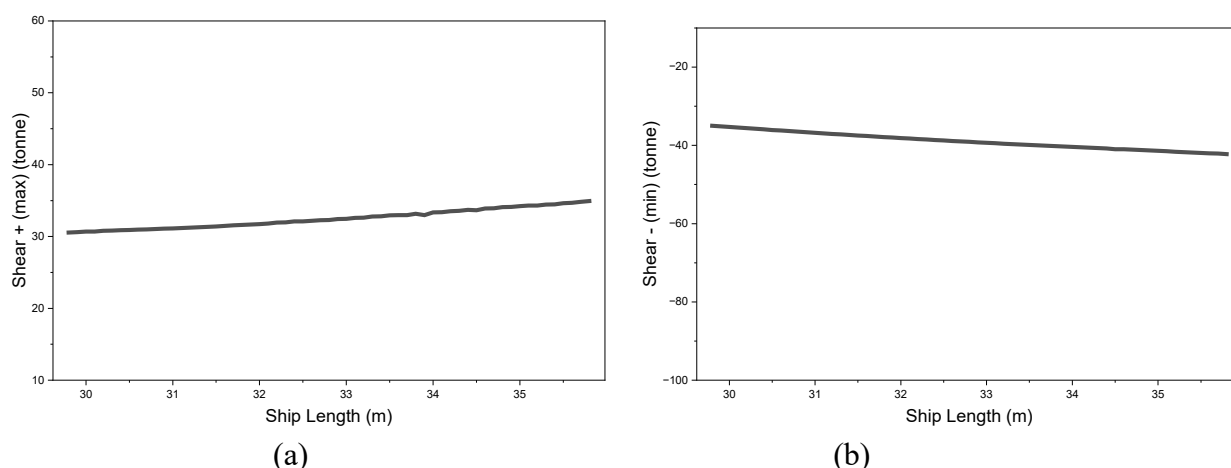


Figure 9 (a) Maximum positive and (b) maximum negative stress by length variant.

3.4 Resistance and running attitude

Figures 10a - 10b present the service condition resistance response across the full set of PMB length variants. A clear monotonic decrease is observed in the total resistance coefficient, as hull length increases (**Figure 10a**), indicating that the adopted lengthening strategy provides systematic resistance benefits within the investigated envelope. The accompanying decomposition shows that the dominant contributor to this reduction is the residuary component, (**Figure 10b**), which decreases more markedly with length than the viscous-related terms.

This interpretation is consistent with the trends in **Figure 11**. The frictional resistance coefficient remains nearly invariant across the length variants (**Figure 11a**), with only a marginal change consistent with Reynolds-number effects, while the correlation-resistance coefficient exhibits a small upward drift (**Figure 11b**). Taken together, **Figures 10** and **11** indicate that the net improvement in is primarily attributable to reduced residuary (wave-related) resistance rather than to changes in viscous resistance, which is comparatively insensitive to the modest geometric intervention imposed by PMB extension.

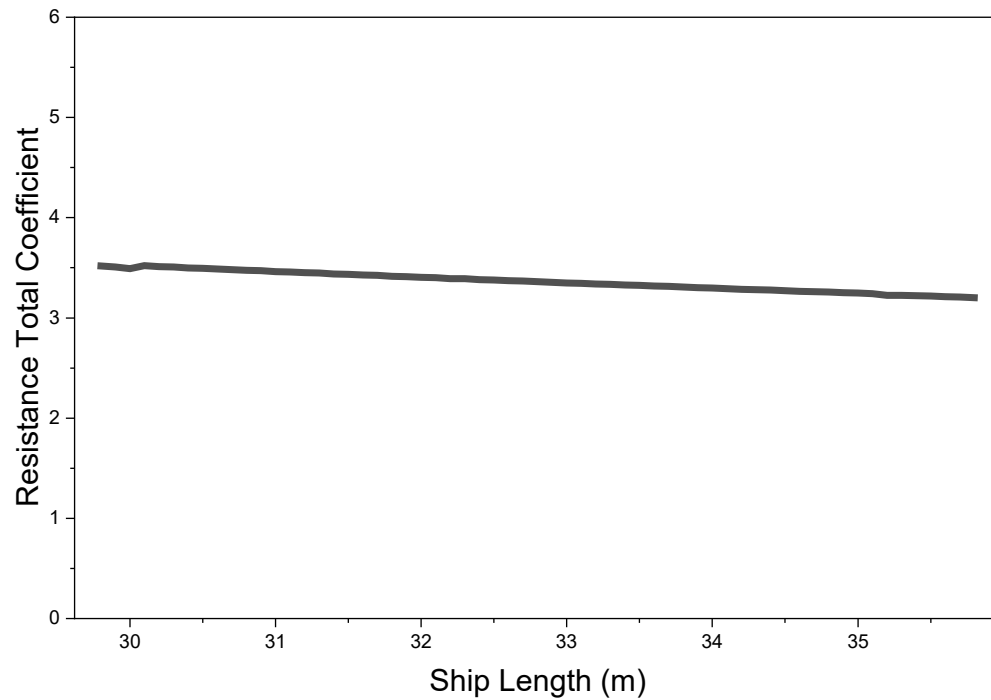
To avoid a single-point interpretation, and to clarify the Froude number regimes in which lengthening is most beneficial, **Figures 10c - 10d** extends the comparison to a Froude-number sweep for three representative configurations: the baseline hull (L = 29.8 m), the selected optimum (L = 35.4 m), and the maximum-length variant (L = 35.8 m). Across the examined range, the lengthened variants maintain lower total and residuary resistance levels than the baseline, with the largest separation occurring in the low to moderate Froude region highlighted in the insets (**Figures 10c - 10d**). Differences between the 35.4 and 35.8 m variants are comparatively small, suggesting diminishing returns as the extension approaches the upper bound of the defined design space.

Figure 10(d) indicates that the residuary resistance coefficient, (C_r), varies smoothly with Froude number over the investigated interval ($Fr = 0.1 - 0.40$), and does not exhibit a pronounced hump hollow pair within this range. Across the same regime, PMB lengthening yields a consistent downward shift in C_r for the lengthened variants relative to the baseline, confirming reduced wave-related (residuary) resistance under equal comparisons of (at equal / at the same) Fr and supporting the interpretation that the total-resistance benefit is primarily residuary driven. This finding is operationally relevant because the craft’s typical operating envelope lies in the low-to-moderate Froude regime; thus, the observed reductions in C_r across $Fr = 0.1 - 0.40$ directly contextualize the service-condition improvements reported in **Figures 10a - 10b** and align with the favorable running-attitude trends discussed subsequently.

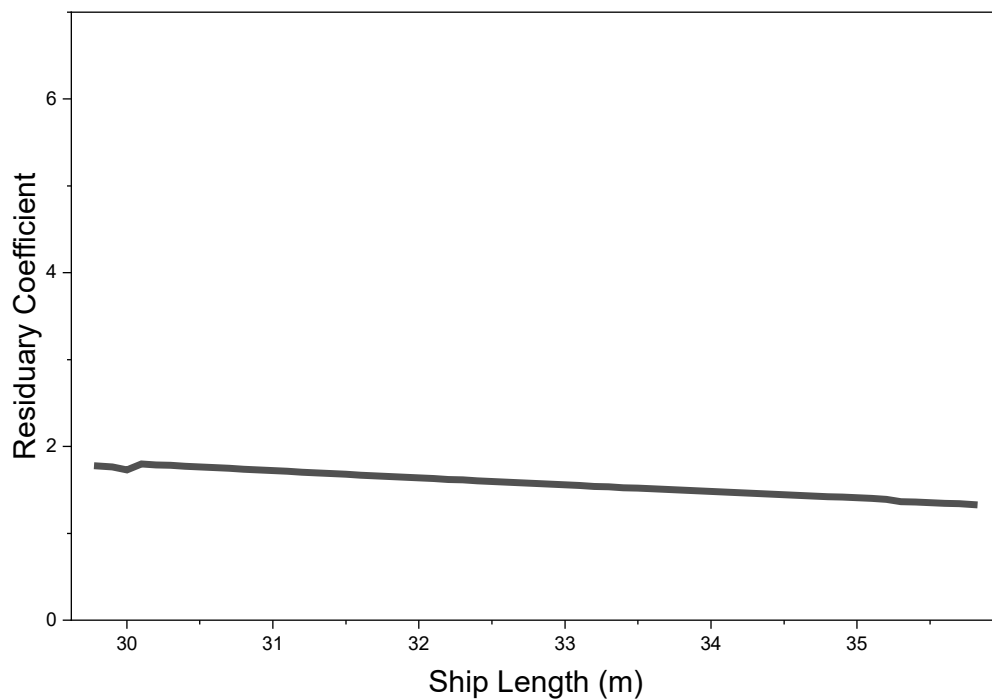
Finally, the predicted running attitude remains favorable as length increases. **Figure 12** shows a progressive reduction in dynamic trim at the service condition (Drouet et al., 2017), indicating a more stable longitudinal equilibrium consistent with the observed resistance improvements and supporting the suitability of PMB extension as a performance-refinement strategy within the study’s constraints.

Table 2 Data frame classification scheme used in the Machine Learning pipeline.

Number	Column	Non-null count		Dtype
0	nan	61	non-null	float64
1	Cw	61	non-null	float64
2	Cp	61	non-null	float64
3	Cb	61	non-null	float64
4	L/B	61	non-null	float64
5	L/T	61	non-null	float64
6	DLR	61	non-null	float64
7	GMt	61	non-null	float64
8	GZ (0-30)	61	non-null	float64
9	GZ (>30)	61	non-null	float64
10	Moment -	61	non-null	float64
11	Shear +	61	non-null	float64
12	Shear -	61	non-null	float64
13	R total Coef.	61	non-null	float64
14	Residuary Coef.	61	non-null	float64
15	Friction Coef.	61	non-null	float64
16	Correlation Coef.	61	non-null	float64
17	Trim (deg)	61	non-null	float64



(a)



(b)

Figure 10 Resistance characteristics for PMB-lengthened variants shown against hull length and Froude number: (a) Total resistance coefficient C_t at the service condition for all 61 variants; (b) Residuary resistance coefficient C_r at the service condition for all 61 variants; (c) C_t-Fr , and (d) C_r-Fr for three representative configurations (baseline $L = 29.8$ m, optimum $L = 35.4$ m, maximum $L = 35.8$ m) evaluated at equal Froude numbers over $Fr = 0.10 - 0.40$; insets highlight the low-to-moderate Fr regime (secondary axis: speed in kn).

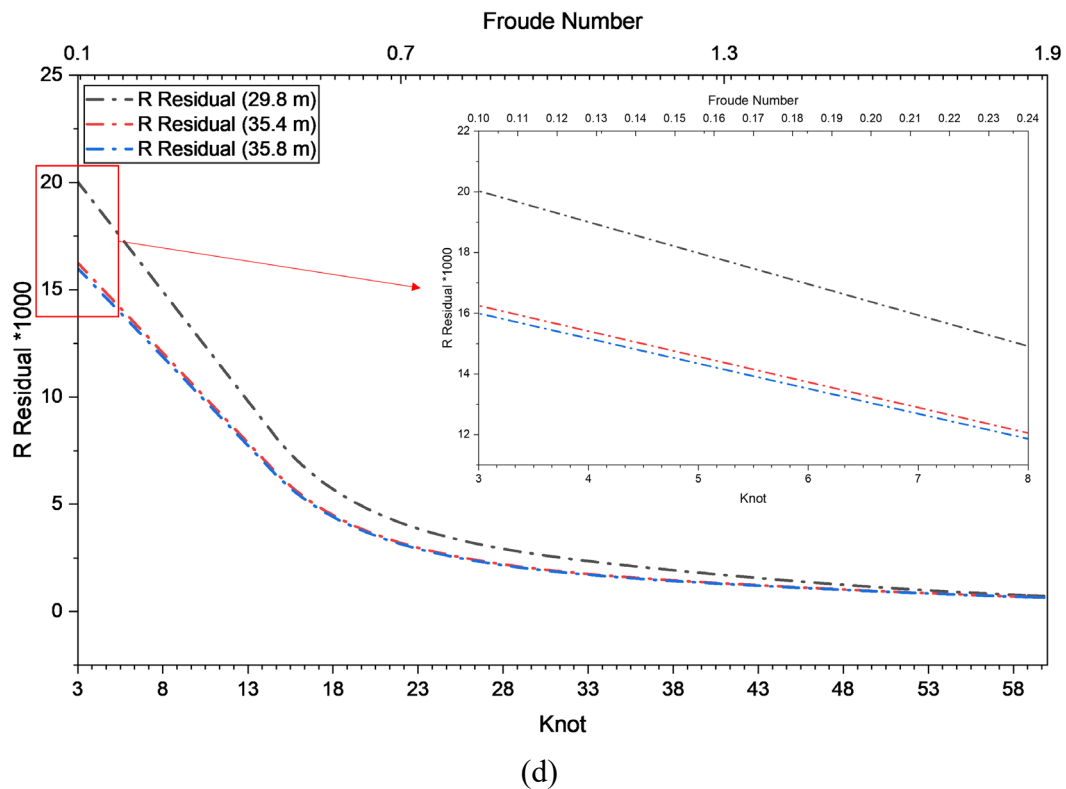
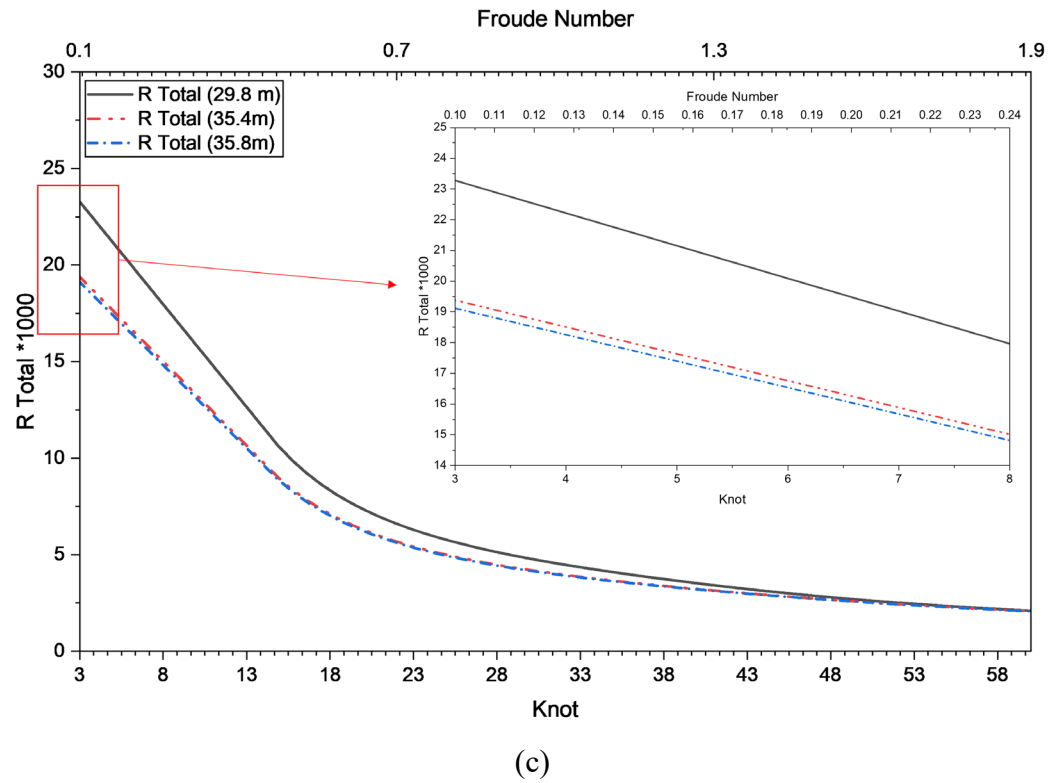


Figure 10 (continued) Resistance characteristics for PMB-lengthened variants shown against hull length and Froude number: (a) Total resistance coefficient C_T at the service condition for all 61 variants; (b) Residuary resistance coefficient C_R at the service condition for all 61 variants; (c) C_T -Fr, and (d) C_R -Fr for three representative configurations (baseline $L = 29.8$ m, optimum $L = 35.4$ m, maximum $L = 35.8$ m) evaluated at equal Froude numbers over $Fr = 0.10 - 0.40$; insets highlight the low-to-moderate Fr regime (secondary axis: speed in kn).

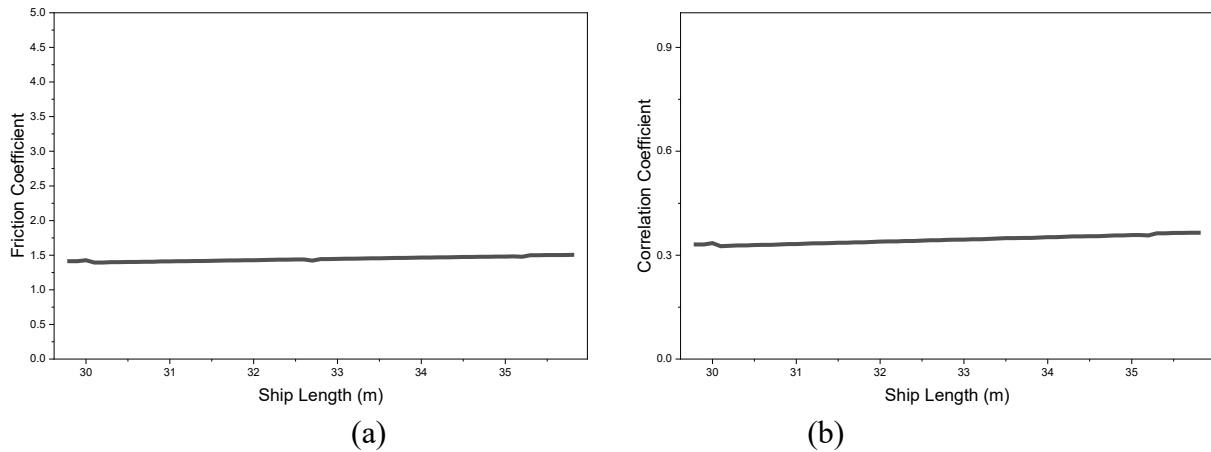


Figure 11 (a) Frictional resistance coefficient by length variant; (b) Correlation-resistance coefficient by length variant.

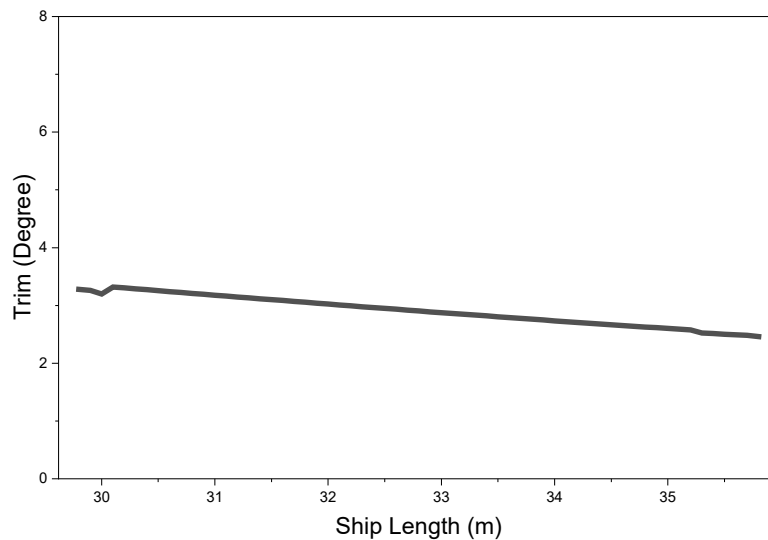


Figure 12 Dynamic trim by stern at service speed for each variant.

3.5 Machine learning performance and optimality identification

The supervised learning framework operationalized here consolidates the dataset into a predictive pipeline against five regressors. Ensemble-based algorithms consistently outperformed linear baselines, with Gradient Boosting identified as the most robust surrogate for capturing nonlinear interactions among geometric and performance descriptors.

Table 3 Verification of training/testing split results.

Data splitting complete	
x_train shape	: (48,17)
x_test shape	: (13,17)
y_train shape	: (48,)
y_test shape	: (17,)

Table 2 presents the classification scheme of the input variables, clarifying how categorical descriptors, such as hull-type identifiers, and continuous descriptors, such as geometric ratios, were systematically organized for modeling (Cui et al., 2018). This classification framework established a transparent basis for subsequent preprocessing steps. The splitting protocol involved a precise allocation of the data: 80 % for training, and 20 % for testing. This rigorous 80 - 20 split, along with the defined type assignments for each variable, ensured both the reproducibility and the validity of the model evaluation (Echeverria et al., 2022). **Table 3** validates representativeness by confirming that the training set preserved the statistical distribution of the full dataset, thereby mitigating risks of sampling bias and enhancing generalizability of the surrogate models (Chicco et al., 2021).

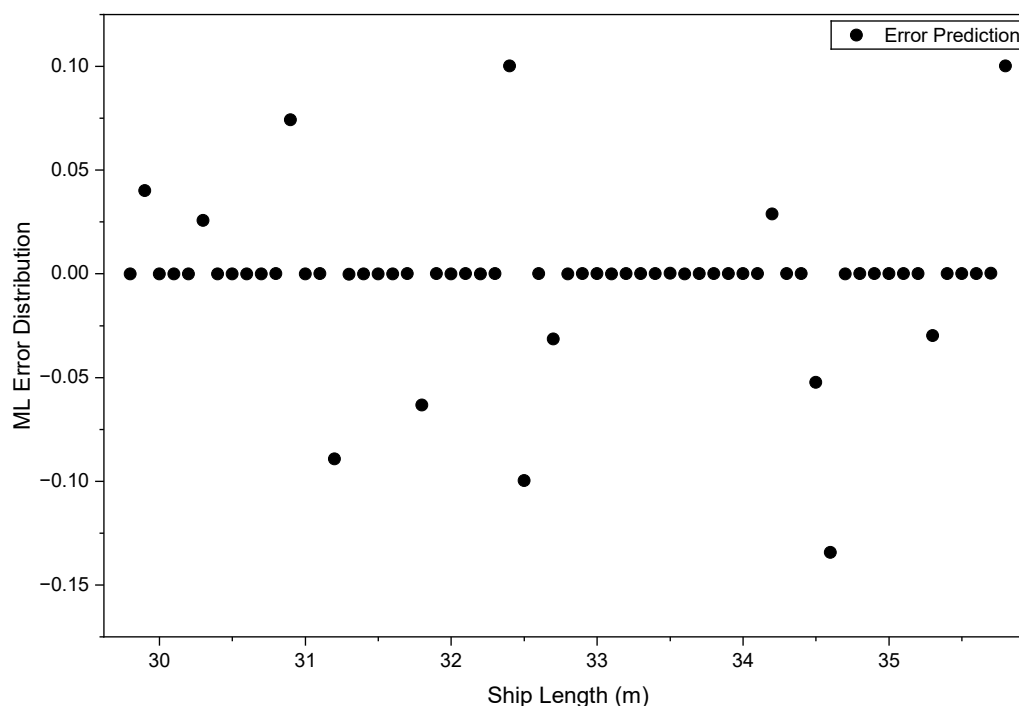


Figure 13 Combined machine learning predictions using 17 ship-parameter features.

Comparative performance across regressors is detailed in **Table 4**, where error metrics (R^2 , MAE, and MSE) reveal a consistent outperformance of tree-based ensembles relative to linear models. **Figure 13** extends this comparison by incorporating all 17 ship-parameter features, illustrating how the ensemble learners retained predictive stability under multicollinearity and achieved improved robustness (Chicco et al., 2021). Convergence dynamics are documented in **Table 5**, which charts the progressive reduction and eventual stabilization of prediction error in Gradient Boosting iterations, evidencing both efficiency and reliability. These temporal dynamics are complemented by **Figure 14**, which depicts the learning trajectories of all five tested regressors. Among them, Gradient Boosting displays the smoothest convergence and lowest residual variance, underscoring its suitability for complex naval-architectural datasets.

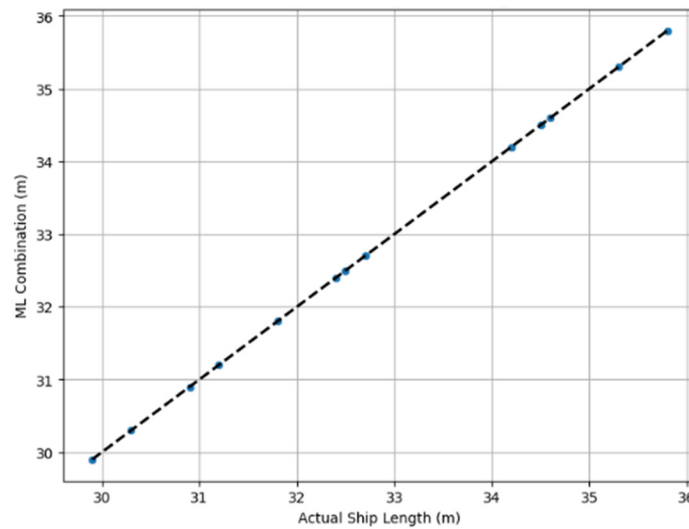
Finally, **Figure 15** synthesizes the optimization outcomes, listing the design candidates ranked through multi-criteria scoring that weighted resistance, stability, and structural strength in balance. This ranking highlights not only the optimal candidate but also provides a transparent hierarchy for secondary alternatives, thus supporting robust design decisions.

Table 4 Predictive model results across algorithms.

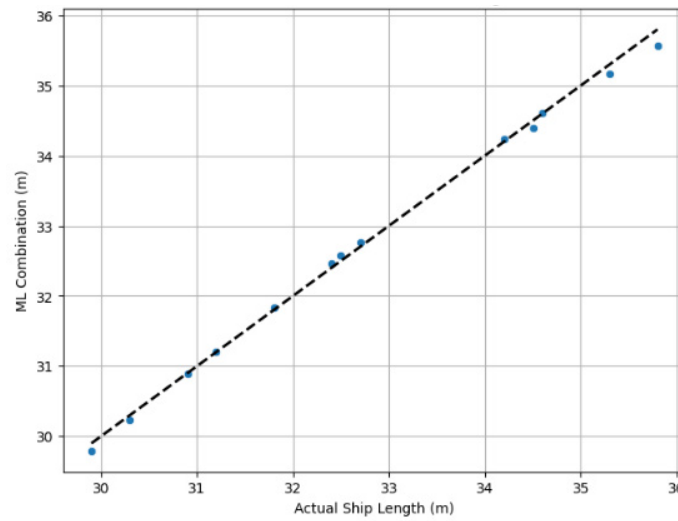
Model Evaluation Results		
Linear Regression		
MAE	:	0
MSE	:	0
R-squared	:	1
Ridge		
MAE	:	0.0732
MSE	:	0.0091
R-squared	:	0.9974
Lasso		
MAE	:	0.2470
MSE	:	0.0975
R-squared	:	0.9975
Random Forest		
MAE	:	0.0725
MSE	:	0.0088
R-squared	:	0.99975
Gradient Boosting		
MAE	:	0.0669
MSE	:	0.0056
R-squared	:	0.9984

Table 5 Gradient Boosting model lapsing/learning summary.

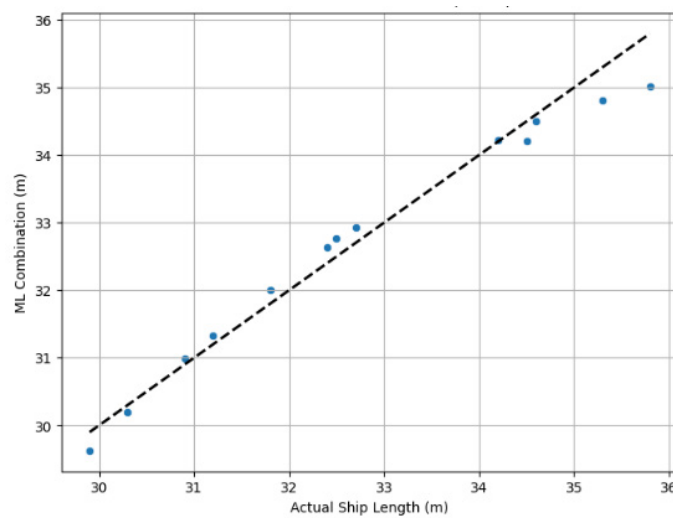
Statistic	Prediction Error
count	61
mean	-0.00215
std	0.03488
min	-0.13428
25 %	-0.00009
50 %	0
75 %	0.00008
max	0.10024



(a)

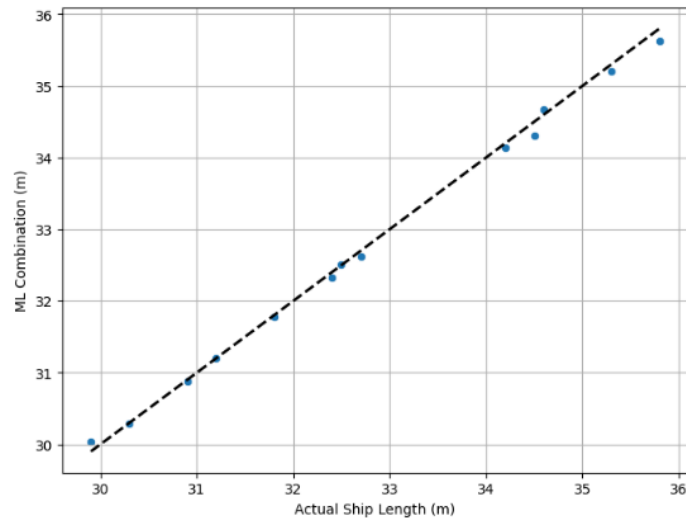


(b)

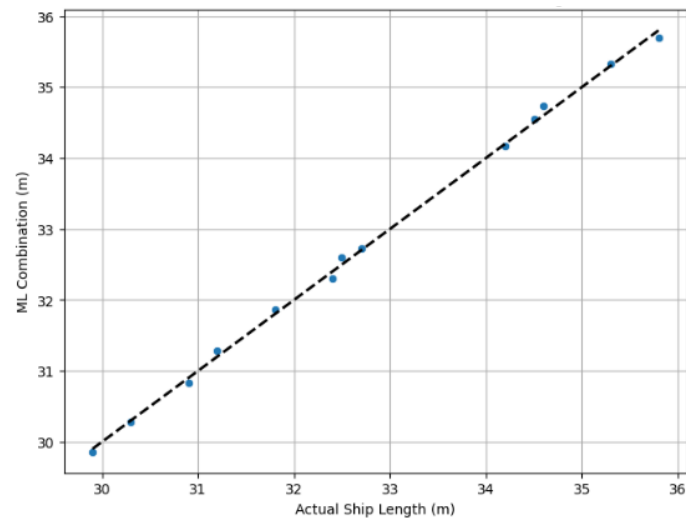


(c)

Figure 14 (a) Train model Linear Regression; (b) Train model ridge; (c) Train model Lasso; (d) Train model Random Forest, and (e) Train model Gradient Boosting.



(d)



(e)

Figure 14 (continued) (a) Train model Linear Regression; (b) Train model ridge; (c) Train model Lasso; (d) Train model Random Forest, and (e) Train model Gradient Boosting.

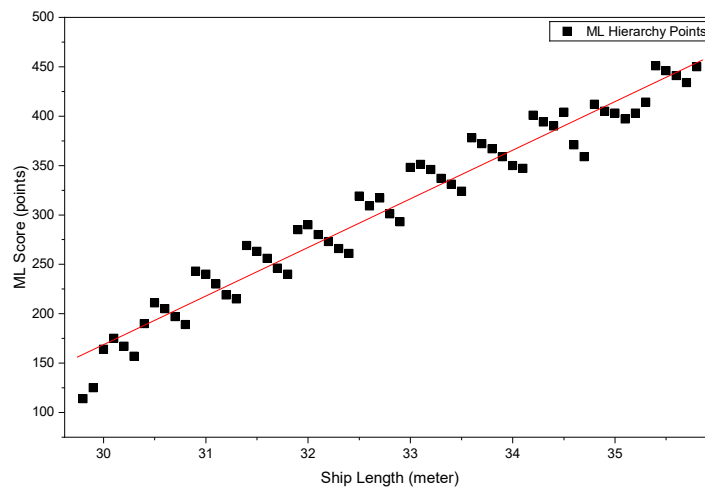


Figure 15 Hierarchy based on ranking and scoring optimization.

The synthesis of ML predictions with baseline computations confirms that Gradient Boosting affords both accuracy and interpretability, enabling a multi-criteria score that balances resistance, stability, and strength. This integrative framework not only accelerates concept-stage decision-making but also underscores the strategic role of hybrid data-driven and physics-based approaches in naval architectural design exploration.

4. Discussion

The present investigation demonstrates that incremental extensions of the parallel middle body (PMB) in fast passenger monohulls yield systematic, cross-domain benefits that reinforce one another in hydrostatics, intact stability, longitudinal strength, and calm-water resistance. The geometric indicators progressive increases in L/B and L/T ratios, modest growth in C_w and C_p , and a corresponding decline in C_b corroborate the transition to a slenderer hull form. This redistribution of underwater volume enhances buoyancy distribution and waterplane inertia, producing hydrodynamic conditions favorable to stability and resistance reduction. Such findings are consistent with canonical principles of high-speed craft design, wherein hull slenderness and judicious volume placement attenuate wave-making resistance and moderate dynamic trim, provided that increases in wetted surface are carefully managed (Blount & McGrath, 2009; Huynh & Tran, 2023).

Stability analysis reveals a coherent pattern: the rise in GMT values, coupled with expansion of GZ-areas at both small and large heel angles, signifies improvements in both initial and reserve stability. Mechanistically, increased C_w augments the waterplane moment of inertia, strengthening the vessel's restoring capacity at small angles, while redistribution of longitudinal volume supports enhanced righting capability at larger heel angles. These results are consistent with classical intact-stability frameworks and contemporary studies linking hull geometry to transverse stability in high-speed passenger vessels (Pawłowski, 2017; Begović et al., 2020). Crucially, these gains were not accompanied by adverse dynamic behaviors; rather, observed reductions in stern-down trim underscore a positive interaction between longitudinal running attitude and transverse stability (Hadler et al., 2007; Helmore et al., 2010).

From a structural perspective, the progressive smoothing of bending-moment distributions and the bounded magnitude of peak stresses confirm that moderate PMB-based lengthening does not compromise longitudinal strength margins. This finding aligns with evidence that geometric alterations primarily affecting load distribution, rather than absolute load magnitudes, can enhance structural robustness (Ivanov, 2007). Furthermore, it resonates with experimental and numerical validation studies showing that structural predictions can achieve close correspondence with experimental data when methodological artifacts such as ventilation are mitigated (Avci & Barlas, 2018). Nonetheless, it must be emphasized that the current analysis was confined to preliminary design fidelity; detailed scantling verification and fatigue assessments remain essential in subsequent design stages (Mohammed et al., 2016; Park & Cho, 2023; Tatsumi et al., 2022).

The resistance results in Section 3.4 indicate that PMB lengthening reduces total resistance primarily through a decrease in the residuary component, and that the Froude-number sweep comparison in **Figure 10(d)** provides the appropriate nondimensional basis for interpreting this effect in terms of operating regime.

The Froude-number sweep results in **Figure 10(d)** provide a regime-based lens for interpreting the residuary resistance coefficient C_r , and for situating the present findings relative to the classical hump hollow behavior reported for monohull ships. In the broader literature, hump hollow signatures are widely associated with wave-interference mechanisms that intensify as vessels transition from displacement toward semi-displacement operation, commonly over $Fr \approx 0.4 - 0.7$, with a resistance peak ("hump") often occurring near $Fr \approx 0.5$ before C_r decreases again at higher speeds (Honaryar et al., 2021; Zhao et al., 2024; Tamunodukobipi & Nitonye, 2019). The magnitude and location of this peak-trough structure are strongly dependent on hull form, loading, and operating environment, such that the hump and subsequent hollow can vary substantially among designs (Liu

et al., 2023; Honaryar et al., 2021; Bulut, 2025). Within this physical context, the present analysis emphasizes $Fr = 0.1 - 0.40$, i.e., a low-to-moderate regime that precedes the interval in which pronounced hump hollow features are most frequently documented. Consistent with that regime dependence, the measured Cr trends remain smooth over the investigated range and do not exhibit a pronounced local hump-hollow pair; PMB lengthening, therefore, manifests primarily as a systematic downward shift in Cr rather than a clear migration of a dominant hump or hollow. This behavior is physically consistent with prior studies on hull lengthening via parallel middle body extension, which indicate that increasing hull length can reduce wave-making penalties and attenuate resistance peaks in the transition regime, particularly across the broader $Fr \approx 0.4 - 0.75$ band where bow hull wave interactions strengthen and wave-making effects become increasingly dominant beyond about (in this regime) (Iqbal et al., 2025; Hetharia, 2018; Sajedi & Ghadimi, 2020; Ghadimi et al., 2018; Zou et al., 2021). Accordingly, the consistently lower Cr values observed for the lengthened variants within $Fr \approx 0.1 - 0.40$ can be interpreted as an early indication of improved wave-related resistance behavior that precedes the canonical hump region; extending the sweep beyond $Fr = 0.4$ in future work would allow direct quantification of whether PMB lengthening reduces hump amplitude, shifts its location, or both, within the displacement to semi-displacement transition.

Beyond providing a mechanism-based interpretation, this framing also clarifies the scope limitation of the present sweep: the results demonstrate robust improvement in the pre-transition regime and motivate a targeted extension of the analysis into $Fr \geq 0.4$, where hump hollow features, if present for the baseline hull, would be expected to emerge most distinctly, and where the lengthening effect on peak amplitude and location can be quantified directly. These regime-based observations also align with prior empirical/analytical work and CFD based validations indicating that relative resistance trends remain robust when geometry is systematically controlled (Islam et al., 2022; Lin et al., 2020), while acknowledging that shallow-water effects can substantially modify resistance and trim and, therefore, require dedicated validation for confined waterways.

A central intellectual contribution of this study is its integration of supervised learning as a surrogate for length-performance mapping within a transparent, multi-criteria decision framework. The superior performance of tree-based ensemble methods, and particularly Gradient Boosting, corroborates trends reported in maritime ML applications for resistance prediction and concept design (Ao et al., 2022; Hasan et al., 2025). The literature emphasizes two key avenues for advancing such surrogates: (i) assembling broader, heterogeneous training corpora to reduce overfitting and covariate shift, exemplified by emerging datasets of tens of thousands of hull forms (Bagazinski & Ahmed, 2023); and (ii) embedding physical insight via physics-informed features, transfer learning from synthetic simulations, and weakly nonlinear analytical models to improve both accuracy and data efficiency (Mavroudis & Tinga, 2025; Feng et al., 2025). The Gradient Boosting surrogate employed here reflects these principles by capturing nonlinear dependencies across geometric descriptors and multi-domain performance indicators.

Recent scholarship further suggests that ensemble methods can be enhanced through hybridization with deep neural networks or attention mechanisms, enabling simultaneous capture of global form trends and localized flow phenomena (Hassanat et al., 2024). In parallel, the increasing uptake of explainable AI tools such as SHAP values or permutation importance offers pathways for elucidating feature contributions in maritime ML applications (Chicco et al., 2021). Embedding such interpretability frameworks would be particularly valuable in safety-critical and regulatory contexts, where transparent justification of ML-driven recommendations is paramount. This opens an avenue for future research integrating hybrid ensemble-deep learning architectures with explainability-oriented analytics to complement the surrogate framework established here.

Positioned within the broader landscape of design automation, the present pipeline comprising PMB parametric edits, empirical and semi-empirical evaluations, and ML surrogates sits alongside alternative paradigms that combine CFD, reduced-order modeling, and advanced optimizers. Bayesian optimization frameworks, for example, integrate CFD-based evaluations with iterative

surrogate updates to navigate expansive design spaces with high efficiency (Wei et al., 2023). Generative models and autoencoders represent an alternative trajectory, directly proposing hull-form variants in latent spaces subsequently screened by surrogates or CFD (Seo et al., 2024; Trinh et al., 2024). The present approach prioritizes interpretability and seamless integration with conventional naval-architectural analyses, attributes particularly valuable during concept design. Future efforts could hybridize these strategies by initiating searches in learned latent spaces and refining candidate geometries using physics-guided surrogates and selective CFD verification.

At the operational level, the implications of PMB-based lengthening extend beyond design, intersecting with energy-efficiency regulations and fleet performance management. Lower resistance at a fixed service speed directly translates to reduced power demand, supporting compliance with emerging EEXI and CII indices, particularly when integrated with operational measures such as optimized routing, hull cleaning schedules, and alternative propulsion strategies (Alshareef & Alghanmi, 2024). Moreover, hybrid physics-data models are increasingly being deployed to predict shaft power dynamically, enabling just-in-time arrivals and other operational adjustments that reinforce efficiency gains realized at the design stage (Mavroudis & Tinga, 2025). This underscores the potential for ML surrogates, when retrained on operational data, to evolve into digital performance companions across the vessel lifecycle.

Nevertheless, limitations warrant acknowledgment. The present study was confined to calm-water analyses of a fast passenger monohull equipped with three water-jets under fixed-speed conditions. Aspects such as seakeeping, maneuverability, appendage-hull interactions, wave-induced structural dynamics, and the sensitivity of stability margins to various operational loading conditions remain unexplored. While empirical and semi-empirical methods were sufficient to cost-effectively analyze 61 variants and train the ML surrogate, high-fidelity CFD or EFD campaigns remain necessary for calibration and for examining performance regimes less well captured by empirical models (Jürgens et al., 2008; Avci & Barlas, 2018; Huynh & Tran, 2023). Similarly, the ranking-and-scoring framework relied on equal or heuristic weighting; future work should incorporate formal multi-objective optimization and uncertainty quantification to expose trade-offs more rigorously, consistent with best practices in design exploration (Smirlis & Bonazountas, 2020).

In conclusion, the PMB-based lengthening strategy evaluated herein exhibits a favorable, multi-domain performance profile, substantiated by both hydrodynamic theory and contemporary design-automation scholarship. The fusion of parametric geometric edits, empirical/analytical assessments, and ML surrogates constitutes a pragmatic and interpretable framework for concept-stage refinement. Advancing this approach toward physics-informed learning, enlarged training datasets, and selective high-fidelity validation will further consolidate its reliability, bridging the gap from conceptual exploration to operational deployment at scale (Bagazinski & Ahmed, 2023; Wei et al., 2023; Bozzo et al., 2025).

5. Conclusions

The investigation has established that systematic elongation of a fast passenger monohull via parallel-middle-body (PMB) extension generates demonstrably favorable outcomes across multiple naval architectural domains, namely, hydrostatics, intact stability, longitudinal strength, and calm-water resistance. Incremental modifications between 29.8 and 35.8 m were shown to produce consistent increases in metacentric height (GMt), expansion of righting-arm areas, and attenuation of bending-moment peaks, while simultaneously yielding reductions in total resistance coefficients driven predominantly by residuary-component moderation.

The integration of these physically grounded results with a supervised machine learning (ML) surrogate, where Gradient Boosting emerged as the most robust and stable regressor, facilitated rapid interrogation of a 61-variant parametric design space and enabled a transparent identification of the optimal length at 35.4 m, which achieved a balanced compromise between resistance reduction, stability enhancement, and strength preservation. This synthesis underscores how controlled

geometric manipulations, supported by empirical and semi-empirical evaluation methods, can be effectively coupled with data-driven surrogates to construct a rigorous and efficient workflow for concept stage hull-form refinement.

Crucially, the outcomes demonstrate that lengthening within the studied bounds augments performance margins without eroding structural integrity, thereby expanding the operational envelope for high-speed service craft. Future research should extend this framework to encompass seakeeping, appendage hull interaction effects, and physics-informed ML approaches in order to consolidate decision support and elevate fidelity at the early design stage.

CRediT author statement

Muhammad Raafie Caesar Putra Hadi: Conceptualization, methodology, investigation, writing original draft, visualization; **Deddy Chrismiarto:** Supervision, formal analysis, review & editing; **Ahmad Firdhaus:** Resources, review & editing; **Eko Sasmito Hadi:** Supervision, data curation, review & editing.

Acknowledgment

The author gratefully acknowledges the Department of Naval Architecture, Faculty of Engineering, Diponegoro University, Indonesia, for providing complimentary access to its laboratory facilities, which greatly supported this research. Additionally, the author thanks the reviewers for their time and valuable comments which helped improve the quality of this manuscript.

References

- Ahn, Y., Lee, J. H., & Kim, Y. (2022). *Application of machine learning for prediction of wave-induced ship motion* (pp. 2067-2071). In Proceedings of the International Offshore and Polar Engineering Conference. International Society of Offshore and Polar Engineers. <https://www.scopus.com/pages/publications/85142160156>
- Alamsyah, A., Fikri, M., Suardi, S., Pawara, M. U., Ikhwan, R. J., Setiawan, W., & Paroka, D. (2024). Comparative assessment of the effect of changing the Breadth (B) of the ship on the stability of the Tugboat. *TransNav*, 18(4), 905-914. <https://doi.org/10.12716/1001.18.04.17>
- Alshareef, M. H., & Alghanmi, A. F. (2024). Optimizing Maritime Energy Efficiency: A machine learning approach using deep reinforcement learning for EEXI and CII compliance. *Sustainability (Switzerland)*, 16(23), 10534. <https://doi.org/10.3390/su162310534>
- Ao, Y., Li, Y., Gong, J., & Li, S. (2022). Artificial intelligence design for ship structures: A variant multiple-input neural network-based ship resistance prediction. *Journal of Mechanical Design*, 144(9), 091707. <https://doi.org/10.1115/1.4053816>
- Avci, A. G., & Barlas, B. (2018). An experimental and numerical study of a high speed planing craft with full-scale validation. *Journal of Marine Science and Technology (Taiwan)*, 26(5), 617-628. [https://doi.org/10.6119/JMST.201810_26\(5\).0001](https://doi.org/10.6119/JMST.201810_26(5).0001)
- Bagazinski, N. J., & Ahmed, F. (2023). *SHIP-D: Ship hull dataset for design optimization using machine learning*. In Proceedings of the ASME Design Engineering Technical Conference. Boston, Massachusetts, USA. <https://doi.org/10.1115/DETC2023-117003>
- Balas, E. A., & Balas, C. E. (2025). Maritime risk assessment: A cutting-edge hybrid model integrating automated machine learning and deep learning with hydrodynamic and Monte Carlo simulations. *Journal of Marine Science and Engineering*, 13(5), 939. <https://doi.org/10.3390/jmse13050939>
- Barhrhouj, A., Ananou, B., & Ouladsine, M. (2025). Exploring explainable machine learning for enhanced ship performance monitoring. *Lecture Notes in Computer Science*, 15509, 1-13. https://doi.org/10.1007/978-3-031-82484-5_1
- Baso, S., Ardianti, A., & Anggriani, A. D. E. (2021). An extended validation of free CFD

- application to ship resistance prediction for using in preliminary design stage. *Journal of Engineering Science and Technology*, 16(3), 2544-2561.
- Baso, S., Bochary, L., Hasbullah, M., Anggriani, A. D. E., & Ardianti, A. (2020). Investigating the performance characteristics of a semi-planing ship hull at high speed. *IOP Conference Series: Materials Science and Engineering*, 875(1), 012076. <https://doi.org/10.1088/1757-899X/875/1/012076>
- Bassam, A. M., Phillips, A. B., Turnock, S. R., & Wilson, P. A. (2022). Ship speed prediction based on machine learning for efficient shipping operation. *Ocean Engineering*, 245, 110449. <https://doi.org/10.1016/j.oceaneng.2021.110449>
- Bassam, A. M., Phillips, A. B., Turnock, S. R., & Wilson, P. A. (2023). Artificial neural network based prediction of ship speed under operating conditions for operational optimization. *Ocean Engineering*, 278, 114613. <https://doi.org/10.1016/j.oceaneng.2023.114613>
- Begović, E., Rinauro, B., & Cakici, F. (2020). *Application of the second generation intact stability criteria for fast semi displacement ships* (pp. 325-331). In Proceedings of the 18th International Congress of the International Maritime Association of the Mediterranean. CRC Press/Balkema.
- Blount, D. L., & McGrath, J. A. (2009). Resistance characteristics of semi-displacement mega yacht hull forms. *Transactions of the Royal Institution of Naval Architects Part B: International Journal of Small Craft Technology*, 151(2), 19-30. <https://doi.org/10.3940/rina.ijst.2009.b2.95>
- Bozzo, S., Ferrando, M., & Villa, D. (2025). Analysis of the virtual towing tank accuracy by means of a new EFD database. *Progress in Marine Science and Technology*, 10, 241-251. <https://doi.org/10.3233/PMST250032>
- Brizzolara, S., Vernengo, G., Pasquinucci, C. A., & Harries, S. (2015). *Significance of parametric hull form definition on hydrodynamic performance optimization* (pp. 254-265). In Muscari, R., Broglia, R., & Salvatore, F. (Eds.). *Computational Methods in Marine Engineering VI*. International Center for Numerical Methods in Engineering. <https://www.scopus.com/inward/record.uri?eid=2-s2.0-84938823078&partnerID=40&md5=ebd5f58bdf19ae4186302a763f24a5e3>
- Bulut, S. (2025). CFD-based keel and stern form optimization of Tirhandils. *Proceedings of the Institution of Mechanical Engineers Part M: Journal of Engineering for the Maritime Environment*, 239(3), 503-518. <https://doi.org/10.1177/14750902251332719>
- Callens, A., Morichon, D., Abadie, S., Delpy, M., & Liquet, B. (2020). Using Random forest and Gradient boosting trees to improve wave forecast at a specific location. *Applied Ocean Research*, 104. <https://doi.org/10.1016/j.apor.2020.102339>
- Chicco, D., Warrens, M. J., & Jurman, G. (2021). The coefficient of determination R-squared is more informative than SMAPE, MAE, MAPE, MSE and RMSE in regression analysis evaluation. *PeerJ Computer Science*, 7, 1-24. <https://doi.org/10.7717/PEERJ-CS.623>
- Cui, X., Bharadwaj, U. R., & Zhou, P. (2018). A framework for multi-criteria decision analysis (Mcdca) applied to conceptual stage of ship design. *Maritime Transportation and Harvesting of Sea Resources*, 2, 897-904.
- Djačkov, V., Žapnickas, T., Čerka, J., Mickevičienė, R., Ašmontas, Ž., Norkevičius, L., Ronkaitytė, I., Zhou, P., & Blanco-Davis, E. (2018). Numerical simulation of a research vessel's aftpart hull form. *Ocean Engineering*, 169, 418-427. <https://doi.org/10.1016/j.oceaneng.2018.09.030>
- Drouet, A., Sergent, P., Causeur, D., & Corrigan, P. (2017). *Trim optimisation in waves* (pp. 592-603). In Proceedings of the 7th International Conference on Computational Methods in Marine Engineering. International Center for Numerical Methods in Engineering.
- Echeverria, F., Leon, M., Esteves, Z., & Redroban, C. (2022). Variation of the intercession

- coefficient used as a hyper parameter in machine learning in regression models. *Communications in Computer and Information Science*, 1547, 3-19.
- Elkafas, A. G., Khalil, M., Shouman, M. R., & Elgohary, M. M. (2021). Environmental protection and energy efficiency improvement by using natural gas fuel in maritime transportation. *Environmental Science and Pollution Research*, 28(43), 60585-60596. <https://doi.org/10.1007/s11356-021-14859-6>
- Fan, A., Wang, Y., Yang, L., Tu, X., Yang, J., & Shu, Y. (2024). Comprehensive evaluation of machine learning models for predicting ship energy consumption based on onboard sensor data. *Ocean and Coastal Management*, 248, 106946. <https://doi.org/10.1016/j.ocecoaman.2023.106946>
- Feng, Y., el Moctar, O., & Jiang, C. (2025). Hydrodynamic optimization of containership design to minimize wave-making and wave-added resistance using a weak-scatterer approach. *Physics of Fluids*, 37(2), 027146. <https://doi.org/10.1063/5.0252310>
- Ferlita, A. L., Ley, J., Qi, Y., Schellin, T. E., Nardo, E. D., El Moctar, O., & Ciaramella, A. (2024). Data-driven model assessment: A comparative study for ship response determination. *Ocean Engineering*, 314, 119711. <https://doi.org/10.1016/j.oceaneng.2024.119711>
- Ferlita, A. L., Qi, Y., Nardo, E. D., El Moctar, O., Schellin, T. E., & Ciaramella, A. (2024). A framework of a data-driven model for ship performance. *Ocean Engineering*, 309, 118486. <https://doi.org/10.1016/j.oceaneng.2024.118486>
- Gafter, R., & Drimer, N. (2021). A design method to assess the primary strength of the delta-type VLFS. *Journal of Marine Science and Engineering*, 9(9), 1026. <https://doi.org/10.3390/jmse9091026>
- Garbatov, Y., & Huang, Y. C. (2020). Multiobjective reliability-based design of ship structures subjected to fatigue damage and compressive collapse. *Journal of Offshore Mechanics and Arctic Engineering*, 142(5), 051701. <https://doi.org/10.1115/1.4046378>
- Ghadimi, P., Sajedi, S. M., & Tavakoli, S. (2018). Experimental study of the wedge effects on the performance of a hard-chine planing craft in calm water. *Scientia Iranica*, 26(3B), 1316-1334. <https://doi.org/10.24200/sci.2018.20607>
- Hadler, J. B., Kleist, J. L., & Unger, M. L. (2007). *On the effect of transom area on the resistance of hi-speed mono-hulls* (pp. 177-184). In Proceedings of the 9th International Conference on Fast Sea Transportation. <https://www.scopus.com/inward/record.uri?eid=2-s2.0-84874160013&partnerID=40&md5=047573a5a591301e4da53c5ed21c9813>
- Hasan, S. M. R., Islam, M. S., Awal, Z. I., & Hossain, K. A. (2025). Prediction and optimization of efficient ship design particulars through advanced machine learning approaches. *Ocean Engineering*, 341(2), 122572. <https://doi.org/10.1016/j.oceaneng.2025.122572>
- Hassanat, A. B., Alqaralleh, M. K., Tarawneh, A. S., Almohammadi, K., Alamri, M., Alzahrani, A., Altarawneh, G. A., & Alhalaseh, R. (2024). A novel outlier-robust accuracy measure for machine learning regression using a non-convex distance metric. *Mathematics*, 12(22), 3623. <https://doi.org/10.3390/math12223623>
- Helmore, P. J., Scott, F. W., & Wong, D. I. H. (2010). *Resistance prediction for round-bilge and hard-chine catamarans* (pp. 278-292). In Proceedings of the International Maritime Conference 2010. <https://www.scopus.com/inward/record.uri?eid=2-s2.0-77954179312&partnerID=40&md5=580f20456706b586a2bce077548df3da>
- Hetharia, W. R., Hage, A., & Rigo, P. (2021). A review of Savitsky pre-planning method to the resistance of semi-displacement passenger ships. *AIP Conference Proceedings*, 2409, 020021. <https://doi.org/10.1063/5.0067984>
- Hetharia, W. R. (2018). Preliminary study on stability parameters of semi-displacement ships. *Applied Mechanics and Materials*, 874, 105-113. <https://doi.org/10.4028/www.scientific.net/amm.874.105>

- Honaryar, A., Ghiasi, M., Liu, P., & Honaryar, A. (2021). A new phenomenon in interference effect on catamaran dynamic response. *International Journal of Mechanical Sciences*, 190, 106041. <https://doi.org/10.1016/j.ijmecsci.2020.106041>
- Huynh, Q. V., & Tran, T. G. (2023). Methods to improve accuracy of planing hull resistance prediction. *Journal of Ship Research*, 67(3), 184-196. <https://doi.org/10.5957/JOSR.05210016>
- Iqbal, M., Trimulyono, A., Samuel, & Mursid, O. (2025). Study of applicability in minimising pitch radius gyration for different hull types to improve seakeeping performance. *Journal of Marine Science and Engineering*, 13(9), 1734. <https://doi.org/10.3390/jmse13091734>
- Islam, H., Ventura, M., Guedes Soares, C., Tadros, M., & Abdelwahab, H. S. (2022). Comparison between empirical and CFD based methods for ship resistance and power prediction. *Marine Technology and Ocean Engineering*, 1, 347-357. <https://doi.org/10.1201/9781003320272-38>
- Ivanov, L. D. (2007). On the relationship between maximum still water shear forces, bending moments, and radii of gyration of the total ship's weight and buoyancy forces. *Ships and Offshore Structures*, 2(1), 39-47. <https://doi.org/10.1533/saos.2006.0147>
- Jürgens, D., Palm, M., Perić, M., & Schreck, E. (2008). *Prediction of resistance of floating vessels* (pp. 19-25). In Proceedings of the RINA - International Conference - Marine CFD 2008. <https://www.scopus.com/inward/record.uri?eid=2-s2.0-55349100218&partnerID=40&md5=00dcffea100048071bf813cc57ec27f5>
- Kanazawa, M., Wang, T., Skulstad, R., Li, G., & Zhang, H. (2023). *Physics-data cooperative ship motion prediction with onboard wave radar for safe operations*. In Proceedings of the IEEE International Symposium on Industrial Electronics. Helsinki, Finland. <https://doi.org/10.1109/ISIE51358.2023.10228113>
- Khazaei, R., Rahmansetayesh, M. A., & Hajizadeh, S. (2019). Hydrodynamic evaluation of a planing hull in calm water using RANS and Savitsky's method. *Ocean Engineering*, 187, 106221. <https://doi.org/10.1016/j.oceaneng.2019.106221>
- Lang, X., Wu, D., & Mao, W. (2022a). Comparison of supervised machine learning methods to predict ship propulsion power at sea. *Ocean Engineering*, 245, 110387. <https://doi.org/10.1016/j.oceaneng.2021.110387>
- Lang, X., Wu, D., & Mao, W. (2022b). *A machine learning ship's speed prediction model and sailing time control strategy* (pp. 3598-3605). In Proceedings of the International Offshore and Polar Engineering Conference. International Society of Offshore and Polar Engineers. <https://www.scopus.com/inward/record.uri?eid=2-s2.0-85141898295&partnerID=40&md5=f79dc3a2049d73e8f50eb3078dd08112>
- Lang, X., Wu, D., & Mao, W. (2021). *Benchmark study of supervised machine learning methods for a ship speed-power prediction at sea*. In Proceedings of the International Conference on Offshore Mechanics and Arctic Engineering. Ocean, Offshore and Arctic Engineering Division. <https://doi.org/10.1115/OMAE2021-62395>
- Le, T. H., Anh, N. D., Tu, T. N., Hoa, N. T. N., & Ngoc, V. M. (2023). Numerical investigation of length to beam ratio effects on ship resistance using ranse method. *Polish Maritime Research*, 30(1), 13-24. <https://doi.org/10.2478/pomr-2023-0002>
- Leal-Ruiz, L. D., Camargo-Díaz, C. P., Paipa-Sanabria, E., Castro-Faccetti, C., & Candelero-Becerra, J. E. (2023). Effect of speed and hull length on the hydrodynamic performance of a semi-planing hull of a shallow-draft watercraft. *Journal of Marine Science and Engineering*, 11(12), 2328. <https://doi.org/10.3390/jmse11122328>
- Lin, D., Prasanta, S. K., & Hamid, H. (2020). Application of michell's integral to high-speed round-bilge hull forms. *Journal of Ship Production and Design*, 36(3), 189-201. <https://doi.org/10.5957/JSPD.08170041>
- Liu, X., Yang, J., Wu, D., Hou, L., Li, X., & Wan, Q. (2023). Numerical analysis of resistance

- characteristics of a novel high-speed quadramaran. *Polish Maritime Research*, 30(2), 11-27. <https://doi.org/10.2478/pomr-2023-0018>
- Ma, M., Paik, J. K., & McNatt, T. (2016). *Hierarchically decomposed multi-level optimization for ship structural design*. In Proceedings of the International Conference on Offshore Mechanics and Arctic Engineering. Ocean, Offshore and Arctic Engineering Division. <https://doi.org/10.1115/OMAE2016-54452>
- Mavroudis, S., & Tinga, T. (2025). Application of transfer learning on physics-based models to enhance vessel shaft power predictions. *Ocean Engineering*, 323, 120540. <https://doi.org/10.1016/j.oceaneng.2025.120540>
- Mohamad Ayob, A. F., Ray, T., & Smith, W. F. (2010). *Hydrodynamic design optimization of a hard chine planing craft for coastal surveillance* (pp. 73-82). In Proceedings of the International Maritime Conference 2010. <https://www.scopus.com/inward/record.uri?eid=2-s2.0-77954199826&partnerID=40&md5=c1f1ac7fe2c63748c13fbbdc2306aa92>
- Mohammed, E. A., Benson, S. D., Hirdaris, S. E., & Dow, R. S. (2016). Design safety margin of a 10,000 TEU container ship through ultimate hull girder load combination analysis. *Marine Structures*, 46, 78-101. <https://doi.org/10.1016/j.marstruc.2015.12.003>
- Montero, F. M., & Valentina, E. D. (2017). *Influence of design choices on seakeeping of motor yachts*. In Proceedings of the Royal Institution of Naval Architects - International Conference on Design and Construction of Super and Mega Yachts 2017. <https://www.scopus.com/inward/record.uri?eid=2-s2.0-85064448015&partnerID=40&md5=6382f8e9f32699f4c8df8bfee095c7e7>
- Paredes, R. J., Plaza, D., Marin-Lopez, J. R., Begovic, E., & Datla, R. (2023). Preliminary assesment of the effect of bottom warp on the dynamics of planing hulls using OpenFOAM. *Proceedings of the International Conference on Offshore Mechanics and Arctic Engineering - OMAE*, 7. Ocean, Offshore and Arctic Engineering Division. <https://doi.org/10.1115/OMAE2023-104777>
- Park, S. H., & Cho, S. R. (2023). *Predicting ship's ultimate longitudinal strength considering the lateral pressure loading* (pp. 393-400). In Proceedings of the 9th International Conference on Marine Structures. CRC Press/Balkema. <https://doi.org/10.1201/9781003399759-43>
- Pawłowski, M. (2017). The stability of a freely floating ship. *Transactions of the Royal Institution of Naval Architects Part A: International Journal of Maritime Engineering*, 159, 1-25. <https://doi.org/10.3940/rina.ijme.2017.al.375>
- Peri, D., & Campana, E. F. (2005). High-fidelity models in global optimization. *Lecture Notes in Computer Science*, 3478, 112-126. https://doi.org/10.1007/11425076_9
- Sajedi, S. M., & Ghadimi, P. (2020). Experimental and numerical investigation of stepped planing hulls in finding an optimized step location and analysis of its porpoising phenomenon. *Mathematical Problems in Engineering*, 2020, 3580491. <https://doi.org/10.1155/2020/3580491>
- Salazar-Domínguez, C. M., Hernández-Hernández, J., Rosas-Huerta, E. D., Iturbe-Rosas, G. E., & Herrera-May, A. L. (2021). Structural analysis of a barge midship section considering the still water and wave load effects. *Journal of Marine Science and Engineering*, 9(1), 1-21. <https://doi.org/10.3390/jmse9010099>
- Samuel, Praja, R. K., Chrismianto, D., Hakim, M. L., Fitriadhy, A., & Bahatmaka, A. (2024). Advancing interceptor design: Analyzing the impact of extended stern form on deep-V planing hulls. *CFD Letters*, 16(5), 59-77. <https://doi.org/10.37934/cfdl.16.5.5977>
- Schirmann, M. L., Gose, J. W., & Collette, M. D. (2023). A comparison of physics-informed data-driven modeling architectures for ship motion predictions. *Ocean Engineering*, 286, 115608. <https://doi.org/10.1016/j.oceaneng.2023.115608>
- Seo, J., Kim, D., & Lee, I. (2024). A study on ship hull form transformation using convolutional

- autoencoder. *Journal of Computational Design and Engineering*, 11(1), 34-48.
<https://doi.org/10.1093/jcde/qwad111>
- Smirlis, Y., & Bonazountas, M. (2020). *A composite indicators approach to assisting decisions in ship LCA/LCC* (pp. 143-150). In Proceedings of the International Conference on Operations Research and Enterprise Systems. Science and Technology Publications.
<https://doi.org/10.5220/0008895401430150>
- Soma, G. C., & Vijayakumar, R. (2023). Hydrodynamic performance of high-speed displacement vessel with hull vane. *Ocean Engineering*, 285(1), 115362.
<https://doi.org/10.1016/j.oceaneng.2023.115362>
- Tamunodukobipi, D., & Nitonye, S. (2019). Numerical analysis of the RAP characteristics of a Catamaran vessel for niger delta pliability. *Journal of Power and Energy Engineering*, 7(10), 1-20. <https://doi.org/10.4236/jpee.2019.710001>
- Tatsumi, A., Iijima, K., & Fujikubo, M. (2022). *Estimation of still-water bending moment of ship hull girder using beam finite element model and ensemble Kalman Filter*. In Proceedings of the Proceedings of the International Conference on Offshore Mechanics and Arctic Engineering. Ocean, Offshore and Arctic Engineering Division.
<https://doi.org/10.1115/OMAE2022-78630>
- Temple, D. W., & Collette, M. (2016). Understanding the trade-offs between producibility and resistance for differing vessels and missions. *Journal of Ship Production and Design*, 32(1), 59-70. <https://doi.org/10.5957/JSPD.32.1.140013>
- Trinh, L. T., Hamagami, T., & Okamoto, N. (2024). 3D ship hull design direct optimization using generative adversarial network. *Journal of Advanced Computational Intelligence and Intelligent Informatics*, 28(3), 693-703. <https://doi.org/10.20965/jaciii.2024.p0693>
- Villa, D., Gaggero, S., Coppede, A., & Vernengo, G. (2020). Parametric hull shape variations by Reduced Order Model based geometric transformation. *Ocean Engineering*, 216, 107826.
<https://doi.org/10.1016/j.oceaneng.2020.107826>
- Wang, H., Zhu, R. C., Xu, D. K., & Li, C. F. (2023). LCG effects on resistance performance of a planing hull in calm water. *Chuan Bo Li Xue/Journal of Ship Mechanics*, 27(6), 803-815.
<https://doi.org/10.3969/j.issn.1007-7294.2023.06.003>
- Wang, P., Chen, Z., & Feng, Y. (2021). Many-objective optimization for a deep-sea aquaculture vessel based on an improved RBF neural network surrogate model. *Journal of Marine Science and Technology (Japan)*, 26(2), 582-605. <https://doi.org/10.1007/s00773-020-00756-z>
- Wei, X., Chang, H., Feng, B., Liu, Z., & Huang, C. (2019). Hull form reliability-based robust design optimization combining polynomial chaos expansion and maximum entropy method. *Applied Ocean Research*, 90, 101860. <https://doi.org/10.1016/j.apor.2019.101860>
- Wei, Y., Sun, G., & Wan, D. (2023). *Hull form optimization using bayesian optimization framework* (pp. 3656-3662). In Proceedings of the International Society of Offshore and Polar Engineers. International Society of Offshore and Polar Engineers.
<https://www.scopus.com/inward/record.uri?eid=2-s2.0-85188741592&partnerID=40&md5=571f3c566cf77caf0c395ee3628d90d1>
- Zhan, Y., Zhang, H., Li, J., & Li, G. (2022). Prediction method for ocean wave height based on stacking ensemble learning model. *Journal of Marine Science and Engineering*, 10(8), 1150.
<https://doi.org/10.3390/jmse10081150>
- Zhang, C., & Mao, X. (2009). Hull form automatic generation based on form parameters. *Wuhan Ligong Daxue Xuebao (Jiaotong Kexue Yu Gongcheng Ban)/Journal of Wuhan University of Technology (Transportation Science and Engineering)*, 33(4), 675-678.
<https://www.scopus.com/inward/record.uri?eid=2-s2.0-70349857663&partnerID=40&md5=5bb0d6fdf56affc5e7c11baa464cb6d7>

- Zhao, Z. L., Yang, B. C., & Zhou, Z. R. (2024). Numerical investigation on a high-speed transom stern ship advancing in shallow water. *Journal of Marine Science and Engineering*, 12(6), 867. <https://doi.org/10.3390/jmse12060867>
- Zheng, Q., Feng, B. W., Liu, Z. Y., & Chang, H. C. (2021). Application of improved particle swarm optimisation algorithm in hull form optimisation. *Journal of Marine Science and Engineering*, 9(9), 955. <https://doi.org/10.3390/jmse9090955>
- Zou, J., Lu, S., Sun, H., Zan, L., & Cang, J. (2021). Experimental study on motion behavior and longitudinal stability assessment of a trimaran planing hull model in calm water. *Journal of Marine Science and Engineering*, 9(2), 164. <https://doi.org/10.3390/jmse9020164>